

Unusual Electron Distribution Functions in the Solar Wind Derived From the Helios Plasma Experiment: Double-Strahl Distributions and Distributions With an Extremely Anisotropic Core

W. G. PILIPP,¹ H. MIGGENRIEDER,² M. D. MONTGOMERY,³ K.-H. MÜHLHÄUSER,¹
H. ROSENBAUER,⁴ AND R. SCHWENN⁴

Electron distribution functions with unusual features, which have been observed on rare occasions in the solar wind by the Helios probes, are presented. Two examples show a strong symmetric bidirectional anisotropy in the energy regime of the halo up to particle energies of 800 eV (double-strahl distributions). Another example shows an unusually strong bidirectional anisotropy in the energy regime of the core (below 150 eV). The infrequently observed double-strahl distributions provide evidence that magnetic field loops can exist in the solar wind where electrons are trapped. In addition, they provide evidence that in the case of electrons trapped in closed magnetic field structures the break in the energy spectrum separating the core from the halo is produced only by collisions. On the other hand, the class of distribution functions with strongly anisotropic cores indicates that in the case of "open" magnetic field lines the break between core and halo is largely determined both by the interplanetary electrostatic potential and by collisions.

1. INTRODUCTION

Propagation of electrons in the solar wind is controlled by the interplanetary magnetic field, the interplanetary electrostatic field, and various scattering processes. The global structure of the magnetic and electric fields and the nature of scattering processes, together with the conditions in the solar corona from which the solar wind electrons emanate, are responsible for the shapes of the electron distribution functions. Therefore, measured details of the observed distribution functions can provide information on these interplanetary propagation conditions.

Electron velocity distribution functions are usually observed in the solar wind to be nearly symmetric about their maxima and nearly isotropic or only moderately anisotropic at low energy ($E < 50$ eV). They may be extremely skewed and anisotropic with respect to the magnetic field direction at larger energies; i.e., they may show a strahl (beam), implying that most energetic electrons move away from the sun with relatively small pitch angles. Some are nearly isotropic at all energies, often showing a slight bidirectional anisotropy. The occurrence of these types of distribution functions is strongly correlated with the sector structure of the magnetic field. Distributions with the strahl occur within the interior of magnetic sectors, whereas nearly isotropic distributions usually occur at sector boundaries [Pilipp *et al.*, this issue (b)].

The distribution functions with a single strahl are qualitatively consistent with present theoretical descriptions for the propagation of electrons in the solar wind (for a review of theoretical considerations, see Pilipp *et al.* [this issue (a)]).

According to these theoretical approaches the electrons propagate along open magnetic field lines reaching from the sun to infinity. Electrons with low kinetic energies (e.g., below 50 eV at a distance of 1 AU) are trapped in an electrostatic potential well if collisions are neglected, but are dragged outward and are effectively scattered by collisions with the protons if Coulomb collisions are taken into account. In contrast, the more energetic electrons overcome the electrostatic potential barrier and escape to infinity, and they are not strongly scattered. These more energetic electrons then propagate outward with relatively small pitch angles, thus forming the strahl. However, the nearly isotropic distribution functions usually observed at sector boundaries have not been derived by such theoretical approaches. Here the electrons appear to be effectively scattered at all energies. The slight bidirectional anisotropies, which are frequently observed for such distributions, may indicate that the electrons are trapped in magnetic field loops, although magnetic mirror effects may also cause bidirectional streaming [e.g., Ogilvie and Scudder, 1981].

Besides these typical electron distribution functions, distributions which differ drastically have been occasionally but quite clearly observed. In spite of their rare occurrence these unusual distributions may more clearly indicate general conditions for electron propagation which are less marked for the more common distributions.

In this paper we present two examples of electron distribution functions observed by the Helios probes which show a strong bidirectional anisotropy at large energies up to several hundred eV (double strahl). In addition we present an example of a distribution function which is characterized by the usual single strahl but which is unusual in that its core at energies below about 100 eV is strongly anisotropic. Electron distributions with bidirectional anisotropies at larger energies (up to several hundred eV) were already observed near the orbit of earth from VELA measurements [Montgomery *et al.*, 1974], from Pronoz 7 measurements [Temny and Vaisberg, 1979], and from ISEE 3 measurements [Bame *et al.*, 1981]. These distributions were observed for time periods starting typically 10 to 20 hours after the passage of shocks and lasting one to two days. The two

¹ Institut für extraterrestrische Physik, Max-Planck-Institut für Physik und Astrophysik, Garching, Federal Republic of Germany.

² Bayerisches Staatsministerium für Landesentwicklung und Umweltfragen, Munich, Federal Republic of Germany.

³ Maxwell Laboratories, Inc., San Diego, California.

⁴ Max-Planck-Institut für Aeronomie, Katlenburg-Lindau, Federal Republic of Germany.

Copyright 1987 by the American Geophysical Union.

Paper number 5A8096.
0148-0227/87/005A-8096\$05.00

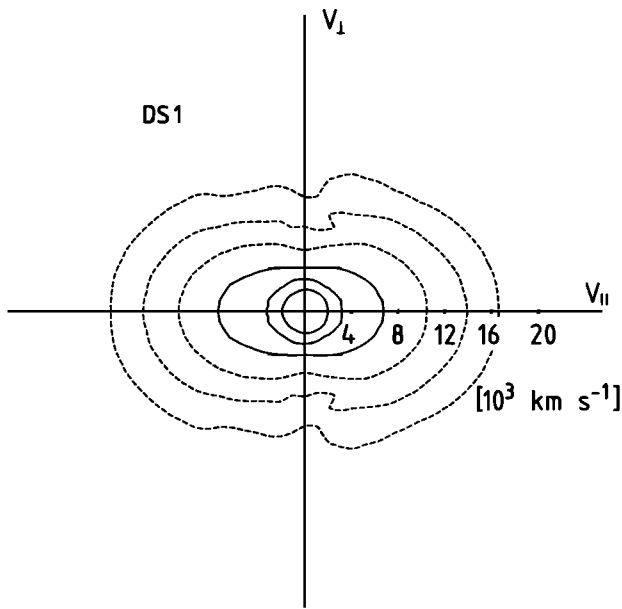


Fig. 1. Contour plot of a double-strahl distribution function, marked with the symbol DS1, which has been observed by Helios 2. The contour lines represent the phase space density within a plane of velocity space parallel to the magnetic field direction and going through the maximum of the distribution function. The coordinate system $(V_{\parallel}, V_{\perp})$ is centered at the electron bulk velocity which is nearly at the maximum of the distribution function (apart from a shift of 35 km s^{-1} along the magnetic field). The V_{\parallel} axis points along the magnetic field. The distribution function is monotonically decreasing with particle energy, and the contour lines are logarithmically spaced corresponding to fractions $10^{-1}, 10^{-2}, \dots, 10^{-6}$ of the maximum phase space density. The dashed lines correspond to count rates smaller than 4 at least in one of the velocity directions along or perpendicular to the magnetic field.

examples of bidirectional anisotropy reported in the present paper were observed at 0.3 AU and 0.8 AU, respectively, where, however, no clear connection with a shock could be seen. Only for one of these examples might a weak shock have occurred half a day before.

The distribution functions reported in the present paper have been determined from measurements which have been performed aboard Helios 1 and Helios 2 during their primary missions or shortly afterward in the years 1975 and 1976, respectively, near solar minimum. The status of the interplanetary plasma during these primary missions has been reported by *Rosenbauer et al.* [1977] for Helios 1 and by *Marsch et al.* [1982] for Helios 2. The method of data analysis used here has been outlined by *Pilipp et al.* [this issue (a)]. The magnetic field data used in this analysis have been provided from the Technische Universität (TU) Braunschweig magnetometer experiment [*Musmann et al.*, 1975, 1977; *Neubauer et al.*, 1977].

2. OBSERVATIONAL RESULTS

In Figure 1 we present the contour plot of an electron distribution function (marked with the symbol DS1) which has been observed by Helios 2 on February 28, 1976, at the distance $R = 0.82 \text{ AU}$ from the sun. It shows a double strahl; i.e., the contour lines are bulged in both directions along the V_{\parallel} axis (parallel to the magnetic field). It should be noted that this distribution function has been constructed from nine cycles of measurements sampled within an observation

time of 5 to 6 min. However, the strong bidirectional anisotropy can be detected in the distributions derived from a single cycle with a time resolution of 18 s also, even though the angular resolution is thereby limited to 45° . (For a description of the Helios electron measurement program, see, for example, *Pilipp et al.* [this issue (a)].)

Figure 2 shows pitch angle distributions for the distribution function DS1 at different kinetic energies E , as seen in a frame of reference moving with the maximum of this distribution function. Here the double strahl shows up within each pitch angle distribution by two peaks, oriented in both directions along the magnetic field (i.e., at $\alpha_p = 0^{\circ}$ and $\alpha_p = 180^{\circ}$). The double-strahl distribution function DS1 shows a relatively well defined core at low particle energies and a halo at higher energies. This can be seen from Figure 3, which shows the electron phase space density $F(E = m(V_{\parallel}^2 + V_{\perp}^2)/2, \alpha_p = \arctan(V_{\perp}/V_{\parallel}))$ as a function of the velocity component V_{\parallel} parallel to the magnetic field at $V_{\perp} = 0$ (solid line on the left-hand plot) and as a function of the perpendicular velocity component V_{\perp} at $V_{\parallel} = 0$ (solid line; right-hand plot), where m is the electron mass. The dashed parabolas represent bi-Maxwellian fits to the low energy part of the distribution function in the energy range from 6 eV to 12 eV or the velocity range from $1.4 \times 10^3 \text{ km s}^{-1}$ to $2 \times 10^3 \text{ km s}^{-1}$ (core fit), and to the high energy part at energies above 71 eV or velocities above $5 \times 10^3 \text{ km s}^{-1}$ (halo fit). The phase space density corresponding to the one-count level is also indicated by dashed lines. The distribution function is statistically significant only if it is well above this one-count level. For mathematical convenience (i.e., in order to avoid $\log F \rightarrow -\infty$) we have extended the distribution function F by

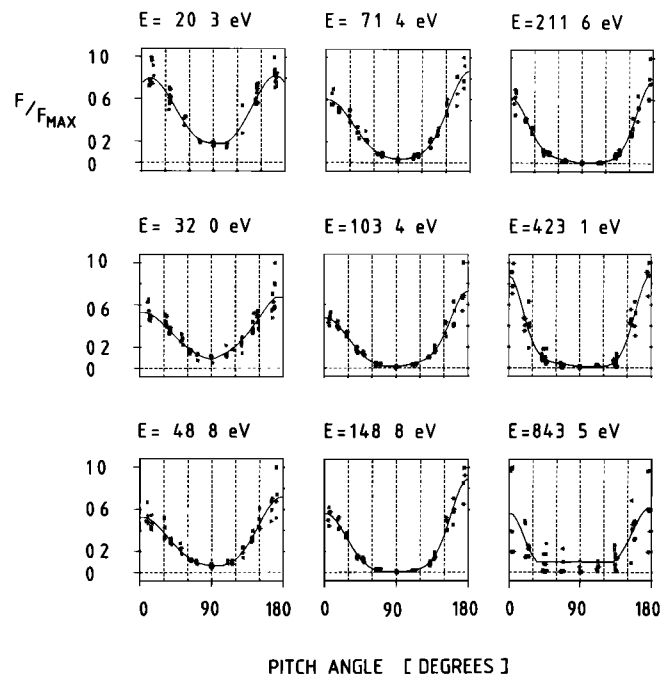


Fig. 2. Pitch angle distributions at different kinetic particle energies E for the distribution function DS1 presented in Figure 1. Each pitch angle distribution shows the phase space density $F(E, \alpha_p)$ in relative units as a function of pitch angle α_p for constant particle energy E , as observed in a frame of reference moving with the maximum of the distribution function. The pitch angle of 0° corresponds to a particle velocity directed parallel to the positive V_{\parallel} axis of Figure 1.

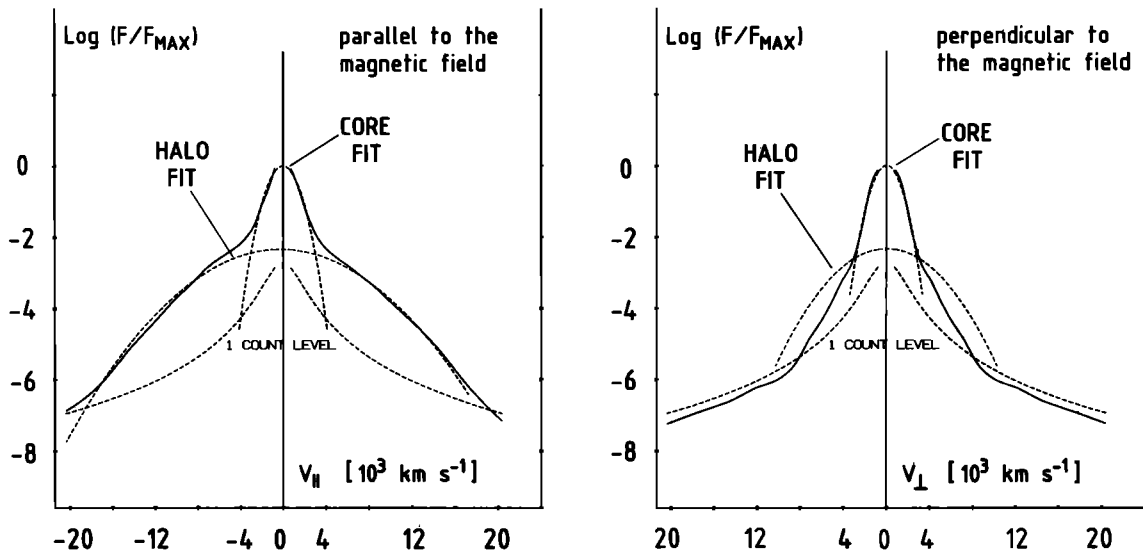


Fig. 3. One-dimensional cuts through the distribution function DS1 (Figure 1) along straight lines in velocity space, which are parallel or perpendicular to the magnetic field and which go through the maximum of the distribution function. The left-hand plot shows the distribution function along a straight line parallel to the magnetic field, and the right-hand plot along a straight line perpendicular to it. Bi-Maxwellian fits to the low energy part (core fit) and to the high energy part (halo fit) as well as the one-count levels are indicated by dashed lines.

a proper extrapolation into the high energy regime where the count rates have been observed to be zero. Here the extrapolated distribution function is below the one-count level.

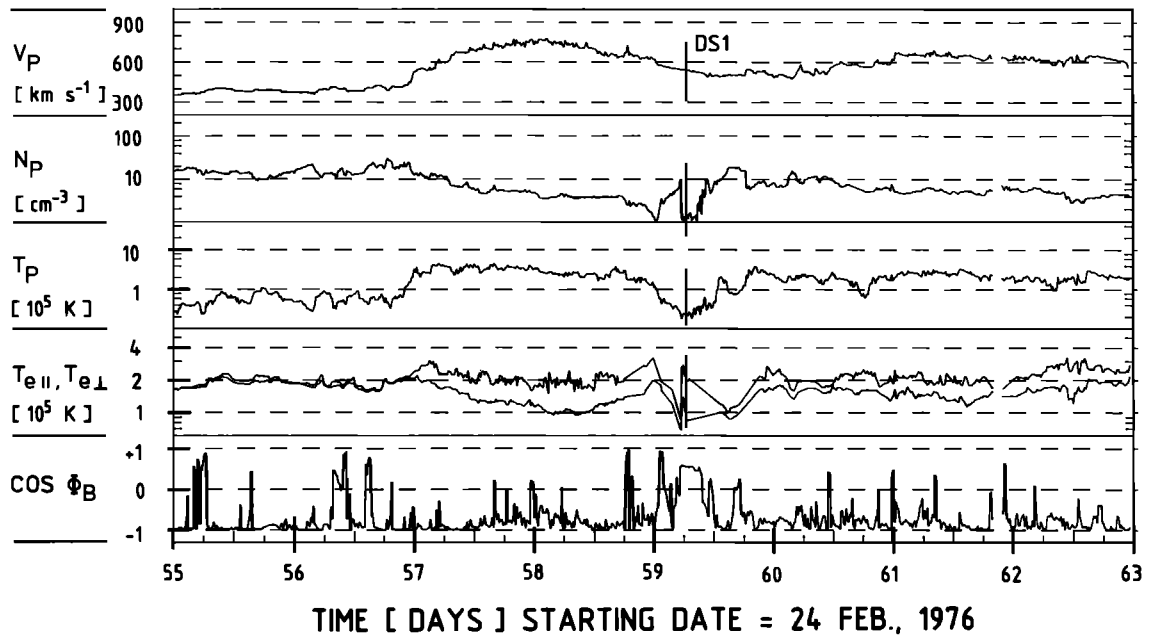
The distribution is well characterized by a cool core at low particle energies and a hotter halo at larger particle energies. The breakpoint energy separating both components is given by the relative sudden change in the slope of the distribution function which occurs for all velocity directions and which agrees roughly with the intersections between core and halo fits. These intersections are at the energies $E_{B1} = 27$ eV and $E_{B2} = 26$ eV for the two velocity directions along the magnetic field, respectively.

The stream structures of the solar wind where the distribution function DS1 has been observed can be seen in Figure 4. Here we have plotted one-hour averages of plasma and magnetic field data as a function of observation time for a time period of 8 days (from February 24 to March 3, 1976). From top to bottom are plotted the proton bulk velocity V_p (which is nearly the solar wind bulk velocity), the proton number density N_p , the proton temperature T_p , and the electron temperatures $T_{e||}$, $T_{e\perp}$ parallel and perpendicular to the magnetic field, respectively. $T_{e||}$ is almost always larger than or equal to $T_{e\perp}$. Only on days 55 and 56 is $T_{e\perp}$ occasionally larger than $T_{e||}$ and then only by a few percent. In the bottom panel we have plotted $\cos \phi_B$, where ϕ_B is the angle between the projection of the magnetic field onto the ecliptic plane and the direction along the Parker spiral away from the sun. The data in the bottom panel characterize the polarity of the interplanetary magnetic field. If $\cos \phi_B = +1$, then the magnetic field is directed outward along the Parker spiral, except for a possible elevation of the magnetic field direction above or below the ecliptic plane. The distribution function DS1 was observed at the end of a high-speed stream in a region of strongly fluctuating density but of a relatively stable magnetic field structure. The density shows a sharp minimum (with $N_p = 1 \text{ cm}^{-3}$) at the observation time of DS1. Also the proton temperature shows a strong depression with

$T_p = 2.4 \times 10^4$ K, and the electron temperatures are $T_{e||} = 2.3 \times 10^5$ K and $T_{e\perp} = 0.9 \times 10^5$ K. The magnetic field polarity has been more or less uniform for a few days before and after the observation time of DS1 but changed for a few hours around the occurrence of DS1. In fact (not shown in the figure), the magnetic field direction was nearly perpendicular to the radial direction for several hours and rotated continuously by about 45° within a plane perpendicular to the radial direction. The magnetic field pressure was larger by more than an order of magnitude than the thermal plasma pressure (proton plus electron pressure). Electron distributions with a similar bidirectional anisotropy were observed within a time period of about 10 hours, starting one or two hours before the occurrence of the distribution function DS1.

Another example of a double-strahl distribution function (marked with the symbol DS2) is shown in Figure 5; it was observed by Helios 1 on March 19, 1975, at 0.32 AU. The corresponding pitch angle distributions are presented in Figure 6. As can be seen from this figure, the pitch angle distributions are practically isotropic at low energies up to 61 eV and show a definite double strahl at energies above 100 eV. This is in contrast to the distribution DS1 where the double strahl is seen at all energies shown in Figure 2 from 20 eV to 800 eV. Figure 7 shows that for the distribution function DS2 also we can clearly distinguish the relatively cool core at low energies from the hotter halo at larger energies. Again defining the breakpoint energy by the intersection between the core fit and the halo fit, which also here is near the change of the slope of the distribution function, we find the breakpoint energies $E_{B1} = 82$ eV and $E_{B2} = 86$ eV for the two velocity directions along the magnetic field, respectively.

The solar wind structures where the distribution function DS2 was observed are shown in Figure 8. Here we have plotted plasma and magnetic field data as a function of observation time for the time period from March 5 to March 13, 1975. Similar to the distribution DS1, the distribution



R [A.U.] 0.85 0.84 0.83 0.82 0.81 0.80 0.79

Fig. 4. The plasma stream structures and the polarity of the interplanetary magnetic field as traversed by the Helios 2 spacecraft from February 24 to March 3, 1976, including the observation time of the distribution function DS1. In order from top to bottom, the parameters correspond to the proton bulk velocity V_p , the proton number density N_p , the proton temperature T_p , the electron temperatures $T_{e||}$, $T_{e\perp}$, and $\cos \phi_B$, where ϕ_B is the angle between the projection of the magnetic field onto the ecliptic plane and the direction along the Parker spiral away from the sun. For the electron temperature, $T_{e||}$ is usually larger than $T_{e\perp}$ when the electron temperature is appreciably anisotropic. Only on days 55 and 56, when the electron temperature is nearly isotropic or only slightly anisotropic, do we sometimes have $T_{e\perp} > T_{e||}$. The observation time of DS1 is indicated by vertical lines and marked with the symbol DS1. The distance R of the spacecraft from the sun is also given.

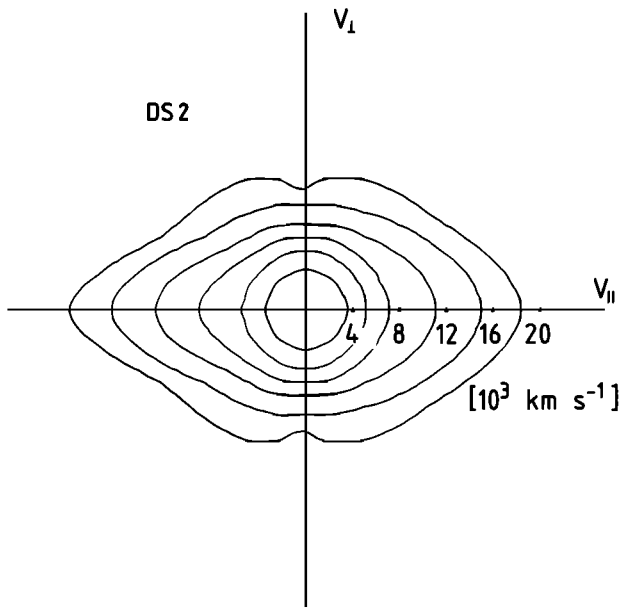


Fig. 5. Contour plot of a double-strahl distribution function (marked with DS2) in a plane of velocity space parallel to the magnetic field and going through the maximum of the distribution function. The coordinate system $(V_{||}, V_{\perp})$ is centered at the electron bulk velocity which is nearly at the maximum of the distribution function (apart from a shift of 55 km s^{-1}). The distribution function DS2 has been observed by Helios 1.

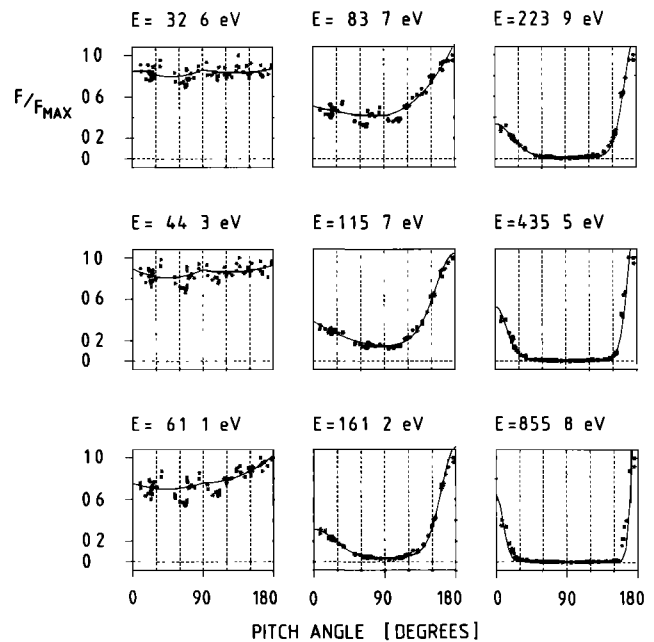


Fig. 6. Pitch angle distributions at different particle energies E for the distribution function DS2 (Figure 5). The particle energies and pitch angles are defined in the maximum rest frame of the distribution function.

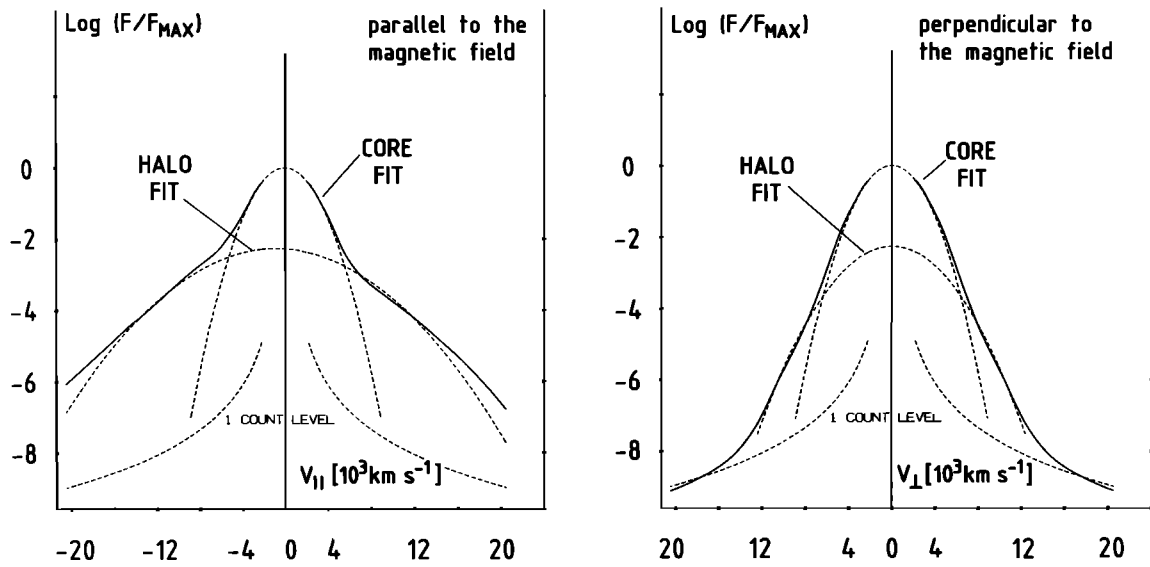


Fig. 7. One-dimensional cuts through the distribution function DS2 (Figure 5) along straight lines in velocity space parallel and perpendicular to the magnetic field and going through the maximum of the distribution function.

DS2 was also observed in a region where the proton temperature is strongly depressed with $T_p = 3.3 \times 10^4$ K. However, in contrast to DS1 the distribution DS2 occurred in a structure resembling a noncompressive density enhancement as described by Gosling *et al.* [1977] with an extremely high proton number density ($N_p = 199 \text{ cm}^{-3}$). The electron temperature was relatively low and moderately anisotropic with $T_{e\parallel} = 1.9 \times 10^5$ K and $T_{e\perp} = 1.7 \times 10^5$ K. As was the case with DS1, DS2 was found in a region where the magnetic field direction was nearly perpendicular to the radial direction for several hours and rotated continuously in

a plane perpendicular to the radial direction by even more than 45° . However, here the magnetic field pressure was only of the same magnitude as the thermal plasma pressure. Similar to DS1, electron distributions with a bidirectional anisotropy could be observed for a time period of several hours, although here this period was interrupted by short time intervals with rather isotropic distributions or distributions with a broad strahl.

Finally, Figures 9, 10, and 11 show a distribution function (marked with DS3) which was observed by Helios 1 at a distance 0.33 AU nearly two days later than the distribution

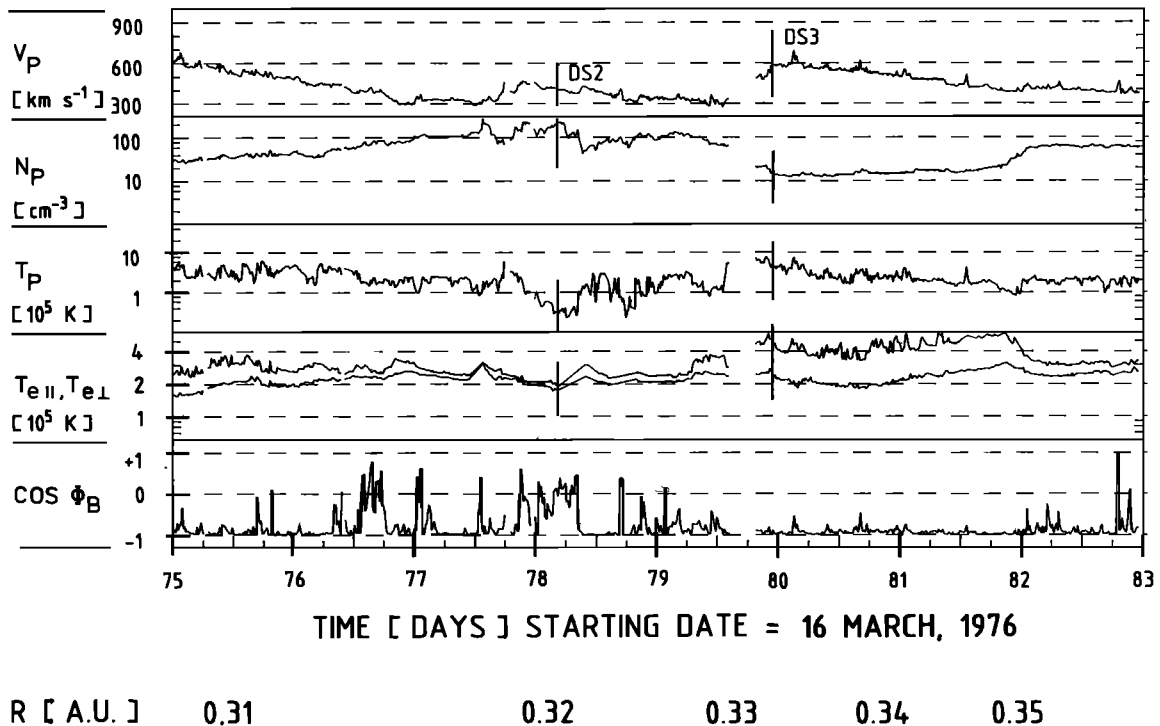


Fig. 8. The plasma stream structures and the polarity of the interplanetary magnetic field traversed by the Helios 1 spacecraft from March 5 to March 13, 1975, including the observation time for the distribution functions DS2 and DS3. The format is identical to that of Figure 4. Here we have always $T_{e\parallel} > T_{e\perp}$.

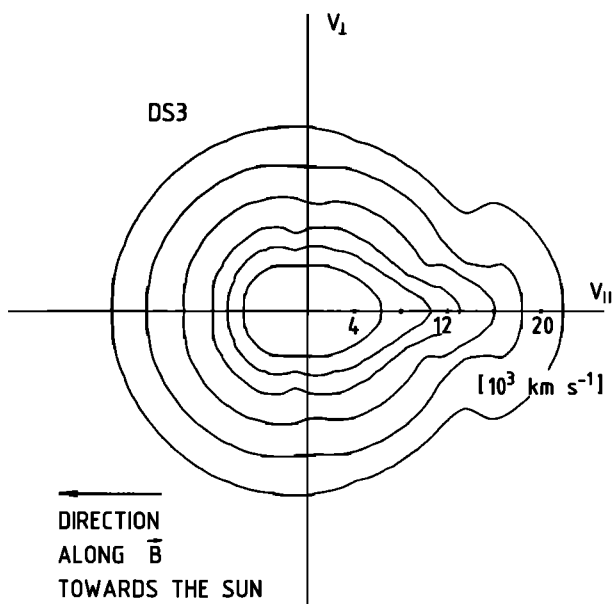


Fig. 9. Contour plot of a distribution function (marked with DS3) with an extremely anisotropic core in a plane of velocity space parallel to the magnetic field and going through the maximum of the distribution function. The coordinate system (V_{\parallel} , V_{\perp}) is centered at the electron bulk velocity which is only slightly shifted along the magnetic field relative to the maximum of the distribution function by 154 km s^{-1} .

function DS2. In contrast to the distribution functions DS1 and DS2, which both show a double strahl at large energies in the halo regime, the distribution function DS3 shows only a single strahl similar to the usual distribution functions with a strahl as presented by Pilipp *et al.* [this issue (a)]. However, the distribution function DS3 is unusual because it is extremely anisotropic in the energy regime of the core and it has a nearly flat top for velocity directions along the magnetic field (see Figure 11). The core fit is poor and yields the extremely high and anisotropic temperatures $T_{e\parallel} = 7.87 \times 10^5 \text{ K}$ and $T_{e\perp} = 2.44 \times 10^5 \text{ K}$, which are even higher and more anisotropic than the temperatures $T_{e\parallel} = 5.1 \times 10^5 \text{ K}$ and $T_{e\perp} = 2.2 \times 10^5 \text{ K}$ found by numerical integration from the entire distribution function. Because of the poor fit of the core temperatures $T_{e\parallel}$ and $T_{e\perp}$ should not be considered representative. However, the core fit is reasonable at low energies, and the high anisotropy of the core temperatures reflects the relatively flat, broad distribution function measured along the direction of the magnetic field.

As is usual for single-strahl distributions, here significant breaks in the slope of the distribution function separating the core from the halo may be discerned only for velocity directions different from the strahl direction. For the velocity direction along the magnetic field toward the sun, i.e., opposite to the strahl, the distribution function agrees roughly with the core fit for particle energies up to 60 eV (or particle velocities up to $4.6 \times 10^3 \text{ km s}^{-1}$) and then drops significantly below this core fit at larger energies. A breakpoint energy E_B or a breakpoint velocity $V_B = (2E_B/m)^{1/2}$, where a sudden change of the slope for the distribution function from a steeper decline at low energies to a flatter decline at larger energies occurs, is discernible for velocity directions along the magnetic field toward the sun and perpendicular to the magnetic field. As judged by the

eye, $V_B \approx 7 \times 10^3 \text{ km s}^{-1}$ to $7.5 \times 10^3 \text{ km s}^{-1}$ or $E_B = 140$ to 160 eV .

As can be seen from Figure 10, each pitch angle distribution shows two peaks with heights of the same order of magnitude for energies $\leq 100 \text{ eV}$, whereas for significantly higher energies there is at most only a very small second peak at the pitch angle of $\alpha_p = 180^\circ$ in addition to the very pronounced peak at $\alpha_p = 0^\circ$.

Similar to distributions DS1 and DS2, the distribution function DS3 was observed in a relatively stable magnetic field structure, where the magnetic field pressure was about 4 times larger than the thermal plasma pressure. However, in contrast to DS1 and DS2, the magnetic field direction was almost radially directed for about two days. In addition, DS3 was observed at the leading edge of a high-speed stream where the proton number density was relatively low ($N_p = 15 \text{ cm}^{-3}$) and the proton temperature was very high ($T_p = 5.4 \times 10^5 \text{ K}$; see Figure 8). Similar distributions were observed for about two days in succession, although the anisotropy of the core was only occasionally this large. Such distribution functions clearly show that the core can become quite anisotropic.

3. DISCUSSION AND CONCLUSION

Electron distribution functions with bidirectional anisotropies in the energy regime of the halo were already observed by Montgomery *et al.* [1974] from VELA and IMP data after some shock events where these distributions were correlated with depressions of the electron temperatures. Montgomery *et al.* interpreted these observations to be likely due to the passage of closed magnetic field structures following flare-induced interplanetary shock waves. Temnyi and Vaisberg [1979] saw from measurements aboard Prognoz 7 strong bidirectional streaming of solar wind electrons along the magnetic field at energies between 50 eV and

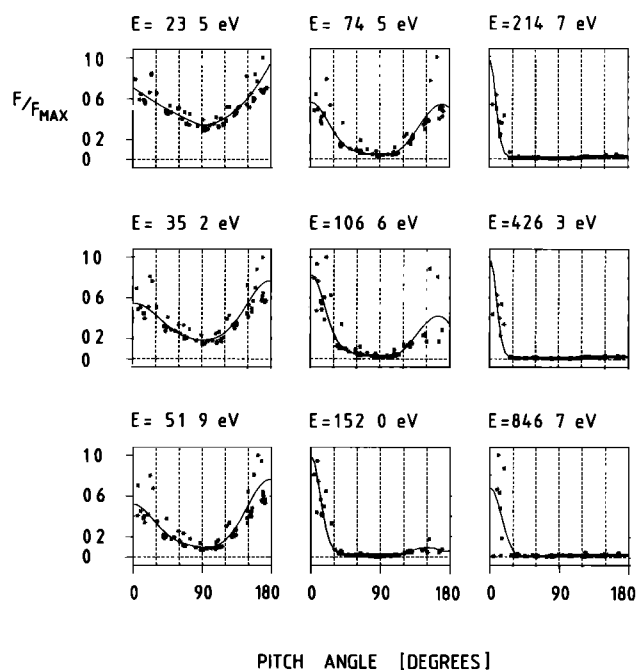


Fig. 10. Pitch angle distributions at different particle energies E for the distribution function DS3 (Figure 9). The particle energies and pitch angles are defined in the maximum rest frame of the distribution function.

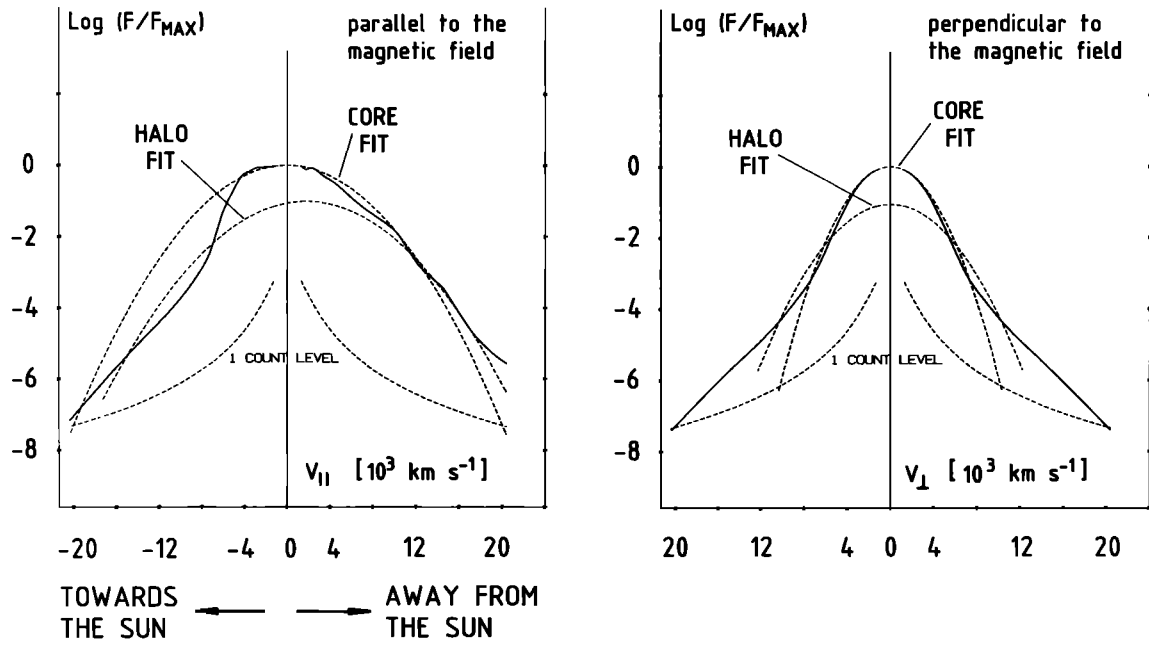


Fig. 11. One-dimensional cuts through the distribution function DS3 (Figure 9) along straight lines in velocity space parallel and perpendicular to the magnetic field and going through the maximum of the distribution function.

200 eV after the passage of a shock wave. They suggested that here the spacecraft was near the top of a magnetic field loop both bases of which rested in the corona. *Bame et al.* [1981] saw, from measurements aboard ISEE 3, strong bidirectional streaming of solar wind electrons at energies above 80 eV in the helium-enriched plasma driving a shock wave. Similarly, these bidirectional distributions were assumed to indicate that the local magnetic field was part of either a magnetic “bottle” rooted at the sun or a disconnected magnetic loop propagating outward. Of course, also the bidirectional distribution functions DS1 and DS2 presented in section 2 may be explained by the assumption of closed magnetic field structures. However, here no clear connection with shock waves could be found. For the distribution DS1 there was no shock discernible within a large period of many days before. For the distribution function DS2, at most a weak shock might have occurred 14 or 15 hours earlier on day 77, at 1345 UT. The magnetic field and plasma data during the time of observation for the distribution function DS1 were very similar to the corresponding data described by *Burlaga et al.* [1981] and *Klein and Burlaga* [1982] for “magnetic clouds” which these authors considered to be expanding magnetic field loops of relatively high magnetic field pressure. Also the magnetic field data during the time of observation of the distribution function DS2 are similar to those for magnetic clouds. But here the thermal plasma pressure was not small compared to the magnetic field pressure.

There are also possible explanations other than closed magnetic field structures for the formation of bidirectional distributions. For example, the electrons may have been mirrored back from a region of larger magnetic field strength [*Ogilvie and Scudder*, 1981]. However, the distributions DS1 and DS2 have not been observed near interaction regions between slow- and fast-speed streams (see Figures 4 and 8), and probably not in connection with shock waves. Thus it

seems not very likely that the distributions DS1 and DS2 occurred near regions where the magnetic field strength increased strongly with distance from the sun. On the other hand, the fact that both distributions DS1 and DS2 were observed in a region where the magnetic field direction was nearly perpendicular to the radial direction is consistent with the hypothesis that these distributions occurred in the outer ends of magnetic loops.

If the two peaks in the pitch angle distributions occur only for energies below the escape energy with respect to the interplanetary electrostatic potential, then there is still another explanation for the formation of bidirectional distributions. The low energy electrons, emanating from the corona and forming a strahl, should be reflected back by the electrostatic potential and thus may form a double-peak distribution, although Coulomb collisions tend to isotropize the distributions. However, for the pitch angle distributions shown in Figures 2 and 6, two peaks occur up to energies of 800 eV, which should be well above the escape energy. In fact, the escape energies determined from the energy balance of the electrons (neglecting magnetic forces) are $E_{T1} \approx E_{T2} \approx 26$ eV for distribution DS1 (with respect to the peak rest frame for the velocity directions along the magnetic field away from and toward the sun, respectively), and $E_{T1} \approx 39$ eV and $E_{T2} \approx 43$ eV for distribution DS2. Thus the distribution functions should be bidirectional only for energies below 26 eV or 43 eV, respectively, if this bidirectional anisotropy is caused by the interplanetary electrostatic field. Therefore the assumption that the electrons have been observed on closed magnetic field line structures seems to be much more plausible.

As has been discussed in more detail by *Pilipp* [1983], electrons traveling on closed magnetic field structures are not always expected to be seen as well-developed double-strahl distributions. Whereas magnetic loops may occur relatively often in the solar wind, the observation of such

symmetric but strongly anisotropic pitch angle distributions as shown in particular in Figure 2 is quite rare. For example, for a survey of Helios 2 data observed within an observation time of three and a half months such double-strahl distributions as shown in Figure 2 have been found only for a time interval of a few hours of observation time. Assume that the spacecraft encounters a magnetic field loop of large size rooted with two foot points at the sun. Then this loop would usually extend outward far beyond the position of the spacecraft. In this more usual case, one foot point at the sun is connected with the spacecraft by a magnetic field line without a detour over solar wind regions much farther away from the sun than the spacecraft. Therefore electrons, having emanated from this foot point and arriving at the spacecraft, have traversed only a distance comparable to the distance of the spacecraft from the sun. If their energy is well above the escape energy with respect to the interplanetary electrostatic potential and if only some minor scattering occurs, these electrons will be observed to propagate outward with small pitch angles. In contrast, electrons emanating from the other foot point could arrive at the spacecraft only via a large detour. In case this detour is comparable to or larger than the effective mean free path due to scattering processes, most of these electrons will be scattered and trapped in the magnetic mirror of the loop, and only a small remnant should arrive at the spacecraft. In addition, if the loop expands in the solar wind, these electrons will be decelerated adiabatically in particular at the outer end of the loop. Then it seems plausible to expect that at the position of the spacecraft the phase space density above the escape energy would be much larger for electrons propagating outward than for inward propagating electrons. In this case we may consider the magnetic field lines to be practically "open," although they may form loops that extend far outward as is often indicated by very small second peaks around the pitch angle $\alpha_p = 180^\circ$ in the pitch angle distributions of the halo.

Double-strahl distributions as presented in section 2 would be observed if, for example, the spacecraft was fortuitously near the outer end of a magnetic loop connected to the sun. Then electrons coming from both foot points have traveled roughly the same distance and thus may form a symmetric distribution function. Also if the spacecraft was at the outer end of a disconnected large scale loop, we expect to observe similar distribution functions.

Since the distribution function DS3 shows only one strahl in the energy regime of the halo, this distribution function should have been observed on practically "open" magnetic field lines. Nevertheless, as has been mentioned in section 2, there seems to be also a very small second peak in the pitch angle distributions at $\alpha_p = 180^\circ$ at energies well above the estimated upper limit of roughly 100 eV for the escape energy with respect to the interplanetary electrostatic potential. This small peak might indicate the presence of closed magnetic field loops, whereby these loops were extending outward far beyond the position of the spacecraft. The very strong bidirectional anisotropy in the core at energies at or below the escape energy could be caused by the interplanetary electrostatic field as discussed above.

As has been discussed by *Pilipp et al.* [this issue (a)], the energy of sudden change in the slope of the distribution functions (breakpoint energy) separating the core from the halo could be determined by the electrostatic potential

and/or the strong energy dependence of the mean free path due to Coulomb collisions or possibly anomalous scattering processes. However, the relative importance of these different mechanisms is not clear and may be different for different distribution functions.

If the break in the slope of the distribution functions is mainly caused by the electrostatic potential as described by exospheric theory, then we expect this break to occur only for velocity directions different from the strahl direction. It is important that the magnetic field lines are assumed to be open in exospheric theory so that the electrostatically unbound electrons at higher energies can escape along the magnetic field lines to infinity and only low energy electrons trapped in the interplanetary electrostatic potential well are reflected back toward the sun. Exospheric theory predicts an exponential decrease of phase space density with particle energy in the velocity direction along the magnetic field away from the sun (i.e., along the strahl), but a sudden drop of phase space density at the escape energy in the velocity direction toward the sun.

Of course, Coulomb collisions will always tend to smear the distribution functions, and a decrease with particle energy along the strahl direction according to a Maxwellian is not expected (see also Figure 5 in the companion paper by *Pilipp et al.* [this issue (a)]). However, if the electrostatic potential is the main cause for the break in the slope of the distributions, then this break should still occur only for velocity directions different from the strahl direction. This is not the case for the double-strahl distributions DS1 and DS2, which show a clear break between core and halo for all velocity directions. Thus we have evidence that the break in these distribution functions may be produced by scattering processes. In fact, if these distribution functions were observed at the outer ends of magnetic field loops as suggested by the symmetry of the double-strahl structure, then the electrons at all energies should be guided toward the sun by the magnetic field. It is hard to see how the interplanetary electrostatic potential could be the cause of the core-halo breaks in these cases.

Assuming that Coulomb collisions are the main mechanism to produce breaks in the slopes of the distribution functions, *Scudder and Olbert* [1979] predict this break to occur at a particle energy of $7\kappa T_c$ in the solar wind rest frame. Here κ is Boltzmann's constant, and T_c is the core temperature. In fact, for the distribution function DS1 we find $7\kappa T_{c\parallel} = 32$ eV and $7\kappa T_{c\perp} = 27$ eV, which are close to the observed breakpoint energies of 26 eV and 27 eV. For the distribution function DS2 we find $7\kappa T_{c\parallel} = 97$ eV and $7\kappa T_{c\perp} = 96$ eV, again reasonably close to the observed breakpoint energies 82 eV and 86 eV. (Since the shifts of the peaks of the distribution functions DS1 and DS2 relative to the electron bulk velocity are only 35 km s⁻¹ and 55 km s⁻¹, respectively, we can neglect the differences between both frames of reference with respect to the breakpoint energies.) On the other hand, as has also been discussed by *Scudder and Olbert* [1979], approximate agreement between $7\kappa T_c$ and the breakpoint energy would even be expected if the interplanetary electrostatic potential were the main cause of the core-halo breaks in the energy spectra. Thus support for the hypothesis, that the core-halo breaks for DS1 and DS2 are caused by collision effects, results mainly from the discrepancies between the observed spectra and those predicted by exospheric theory as discussed above. In contrast to DS1

and DS2, the interplanetary electrostatic potential may well play an important role in determining the break between core and halo in the case of distribution DS3. This conclusion is supported by the fact that in Figure 11 a significant break can be discerned not in the strahl direction but only for velocity directions opposite and perpendicular to it, in qualitative agreement with exospheric theory. In addition, the energy of about 60 eV, above which the distribution function drops below the core fit for the velocity direction opposite to the strahl, and the breakpoint energy E_B of about 140 eV to 160 eV for this velocity direction are in rough agreement (within a factor of 2) with the estimated upper limit of 100 eV for the escape energy with respect to the interplanetary electrostatic potential. Finally, the strong bidirectional anisotropy is restricted to particle energies at or below the estimated upper limit of 100 eV for the escape energy. These observations are consistent with the hypothesis that both the electrostatic potential and Coulomb collisions determine the breakpoint energy. Here the break could mark the boundary between low energy electrons that have been primarily reflected back toward the sun by the interplanetary electrostatic potential and the electrons at higher energy that have been scattered back by collisions only.

Note that the nearly isotropic distribution function with the slight bidirectional anisotropy in the halo as discussed by Pilipp *et al.* [this issue (a)] shows a break between core and halo for all velocity directions, similar to distributions DS1 and DS2, whereas the usual distribution functions with a strahl show this break only for velocity directions different from the strahl direction, similar to the case of distribution DS3. This may be an additional indication that the nearly isotropic distribution functions, as usually observed at sector boundaries, result from electrons trapped in the outer regions of magnetic field loops, whereas distribution functions with a single strahl, as usually observed outside sector boundaries, correspond to electrons on effectively "open" magnetic field lines.

Acknowledgments. A careful reading of a preliminary version of the manuscript by E. Marsch resulting in valuable comments is gratefully acknowledged. We also thank F. Neubauer and his coworkers for making their magnetic field data available for this study. The Helios project is jointly conducted and supported by the German Bundesministerium für Forschung und Technologie (BMFT) and the U.S. National Aeronautics and Space Administration (NASA). The Helios plasma experiment and its data evaluation and scientific interpretation are supported by the BMFT under grants WRS 10/7 and WRS 0108.

The Editor thanks W. C. Feldman and J. D. Scudder for their assistance in evaluating this paper.

REFERENCES

- Bame, S. J., J. R. Asbridge, W. C. Feldman, J. T. Gosling, and R. D. Zwickl, Bidirectional streaming of solar wind electrons >80 eV: ISEE evidence for a closed-field structure within the driver gas of an interplanetary shock, *Geophys. Res. Lett.*, **8**, 173, 1981.
 Burlaga, L., E. Sittler, F. Mariani, and R. Schwenn, Magnetic loop behind an interplanetary shock: Voyager, Helios, and IMP 8 observations, *J. Geophys. Res.*, **86**, 6673, 1981.

- Gosling, J. T., E. Hildner, J. R. Asbridge, S. J. Bame, and W. C. Feldman, Noncompressive density enhancements in the solar wind, *J. Geophys. Res.*, **82**, 5005, 1977.
 Klein, L. W., and L. F. Burlaga, Interplanetary magnetic clouds at 1 AU, *J. Geophys. Res.*, **87**, 613, 1982.
 Marsch, E., K.-H. Mühlhäuser, R. Schwenn, H. Rosenbauer, W. Pilipp, and F. M. Neubauer, Solar wind protons: Three-dimensional velocity distributions and derived plasma parameters measured between 0.3 and 1 AU, *J. Geophys. Res.*, **87**, 52, 1982.
 Montgomery, M. D., J. R. Asbridge, S. J. Bame, and W. C. Feldman, Solar wind electron temperature depressions following some interplanetary shock waves: Evidence for magnetic merging?, *J. Geophys. Res.*, **79**, 3103, 1974.
 Musmann, G., F. M. Neubauer, A. Maier, and E. H. Lammers, Das Förstersonden-Magnetfeldexperiment (E2), *Raumfahrtforschung*, **19**, 232, 1975.
 Musmann, G., F. M. Neubauer, and E. Lammers, Radial variation of the interplanetary magnetic field between 0.3 AU and 1.0 AU, *J. Geophys. Res.*, **42**, 591, 1977.
 Neubauer, F. M., G. Musmann, and G. Dehmel, Fast magnetic fluctuations in the solar wind: Helios 1, *J. Geophys. Res.*, **82**, 3201, 1977.
 Ogilvie, K. W., and J. D. Scudder, Observations of the 'Strahl' by the solar wind electron spectrometer on Mariner 10, in *Solar Wind Four, Rep. MPAE-W-100-81-31*, edited by H. Rosenbauer, p. 250, Max-Planck-Inst. für Aeron., Katlenburg-Lindau, West Germany, 1981.
 Pilipp, W. G., Solar wind electrons as a probe for the global structure of the interplanetary magnetic field, in *Topics in Plasma-, Astro- and Space Physics*, edited by G. Haerendel and B. Battrock, p. 91, Max-Planck-Institut für Physik und Astrophysik, Institut für extraterrestrische Physik, Garching bei München, West Germany, 1983.
 Pilipp, W. G., H. Miggenrieder, M. D. Montgomery, K.-H. Mühlhäuser, H. Rosenbauer, and R. Schwenn, Characteristics of electron velocity distribution functions in the solar wind derived from the Helios plasma experiment, *J. Geophys. Res.*, this issue (a).
 Pilipp, W. G., H. Miggenrieder, K.-H. Mühlhäuser, H. Rosenbauer, R. Schwenn, and F. M. Neubauer, Variations of electron distribution functions in the solar wind, *J. Geophys. Res.*, this issue (b).
 Rosenbauer, H., R. Schwenn, E. Marsch, B. Meyer, H. Miggenrieder, M. D. Montgomery, K.-H. Mühlhäuser, W. Pilipp, W. Voges, and S. M. Zink, A survey on initial results of the Helios plasma experiment, *J. Geophys. Res.*, **42**, 561, 1977.
 Scudder, J. D., and S. Olbert, A theory of local and global processes which affect solar wind electrons, 2, Experimental support, *J. Geophys. Res.*, **84**, 6603, 1979.
 Temnyi, V. V., and O. L. Vaisberg, A dumbbell distribution of epithermal electrons in the solar wind based on observations on the Prognoz 7 satellite, *Cosmic Res.*, Engl. Transl., **17**, 476, 1979. (Translated from *Kosm. Issled.*, **17**, 580, 1979.)

H. Miggenrieder, Bayerisches Staatsministerium für Landesentwicklung und Umweltfragen, Rosenkavalierplatz 2, 8000 München, Federal Republic of Germany.

M. D. Montgomery, Maxwell Laboratories, Inc., 8888 Balboa Avenue, San Diego, CA 92123.

K.-H. Mühlhäuser and W. G. Pilipp, Max-Planck-Institut für Physik und Astrophysik, Institut für extraterrestrische Physik, D-8046 Garching bei München, Federal Republic of Germany.

H. Rosenbauer and R. Schwenn, Max-Planck-Institut für Aeronomie, 3411 Katlenburg-Lindau, Federal Republic of Germany.

(Received May 16, 1985;
 revised July 10, 1986;
 accepted August 14, 1986.)